Photophysical, electrochemical, and mesomorphic properties of a liquid-crystalline [60]fullerene–peralkylated ferrocene dyad†

Stéphane Campidelli,*[ab] Marjorie Séverac,[b] David Scanu,[b] Robert Deschenaux,[b] Ester Vázquez,[cd] Dragana Milic,[de] Maurizio Prato,*[d] Maurizio Carano,[f] Massimo Marcaccio,[f] Francesco Paolucci,*[f] G. M. Aminur Rahman[g] and Dirk M. Guldi*[g]

Received 31st October 2007, Accepted 6th December 2007
First published as an Advance Article on the web 16th January 2008
DOI: 10.1039/b716806c

Two fullerene–peralkylated ferrocene derivatives were synthesized: (1) a liquid-crystalline dyad (compound **1**) was obtained by introduction of nonamethyl ferrocene into a liquid-crystalline fullerene derivative and (2) a reference compound (compound **2**) was synthesized by attachment of nonamethyl ferrocene to a fulleropyrrolidine. The liquid-crystalline dyad displayed an enantiotropic smectic A phase from 57 to 155 °C. Oxidation and reduction processes were investigated by cyclic voltammetry, and were in agreement with the electrochemical characteristics of the redox-active units (peralkylated ferrocene, fullerene, dendrimer). Photoinduced electron transfer from ferrocene derivative to fullerene was identified.

Introduction

Combining electron donor units with [60]fullerene (C_{60}) (electron acceptor) into ordered materials offers a unique opportunity to control the positioning of each subunit at the molecular level.[1–4] In former studies, we, and others, have demonstrated that liquid crystals are excellent candidates for organizing fullerenes within supramolecular structures.[5–11] Notably, we showed that addition of liquid-crystalline addends *via* the *Bingel*[12] or 1,3-dipolar cycloaddition[13,14] reactions on C_{60} leads to self-organized materials[10,11] for which the liquid-crystalline properties of the addend (malonates or aldehydes) are transferred to C_{60} without notable changes in the mesomorphism. This synthetic strategy was also applied to the preparation of liquid-crystalline C_{60} derivatives containing electron donors (*i.e.*, ferrocene,[15–17] oligophenylenevinylene[18] and tetrathiafulvalene[19]). This approach is of particular interest, since such materials spontaneously form ordered assemblies that could be oriented to give high-performance thin films.

Recently, we have described the synthesis of C_{60}-ferrocene[16] and C_{60}-porphyrin[20] electron donor–acceptor conjugates bearing liquid-crystalline dendrimers. While C_{60}-ferrocene exhibited mesomorphic properties—smectic A phase—C_{60}-porphyrin was found to be non-mesomorphic. These two dyads exhibited very interesting electron transfer properties with lifetimes of the charge separated states of the order of several hundred nanoseconds.

We decided to use a similar strategy to incorporate a peralkylated ferrocene (Fc*) into liquid-crystalline C_{60} derivatives. An important incentive is that permethylated ferrocene derivatives are easier to oxidize than less alkylated ferrocenes.[21] Consequently, peralkylated ferrocenes can be used as efficient electron donor moieties in fullerene-based dyads. Herein, we describe the synthesis, characterization and properties of two C_{60}-Fc* dyads **1** and **2**. As shown in Fig. 1, compound **1** contains a second-generation liquid-crystalline dendrimer ensuring mesomorphic properties, while **2**, which lacks a liquid-crystalline promoter, was used as a model compound.

Results and discussion

Synthesis

The synthesis of **1** and **2** is depicted in Scheme 1. Fullerene derivatives **3**[16] and **4**[22] were synthesized in accordance with a previously described literature procedure. In particular, the amino groups in **3** and **4** were quantitatively deprotected with TFA to give **5** and **6**, which were then attached to the peralkylated ferrocene derivative **7** by a coupling reaction in the presence of 1-hydroxybenzotriazole (HOBT) and 1-(3-dimethylaminopropyl)3-ethylcarbodiimide hydrochloride (EDC). The Fc* derivative **7** was synthesized by reacting nonamethylferrocene

[a]*Laboratoire d'Electronique Moléculaire, Service de Physique de l'Etat Condensé (CNRS URA 2464), CEA Saclay, F-91191 Gif sur Yvette Cedex, France. E-mail: stephane.campidelli@cea.fr; Fax: +33-(0)169086640; Tel: +33-(0)169088877*
[b]*Institut de Chimie, Université de Neuchâtel, Avenue de Bellevaux 51, CP 158, CH-2009 Neuchâtel, Switzerland*
[c]*Departamento de Química Inorgánica, Orgánica y Bioquímica, Facultad de Químicas, Universidad Castilla-La Mancha, Ciudad Real, Spain*
[d]*Dipartimento di Scienze Farmaceutiche, INSTM, unit of Trieste, Università degli Studi di Trieste, Piazzale Europa 1, I-34127 Trieste, Italy. E-mail: prato@units.it; Fax: +39-04052572; Tel: +39-0405587883*
[e]*Faculty of Chemistry, University of Belgrade, PO Box 158, 11000 Belgrade, Yugoslavia*
[f]*Università di Bologna, Dipartimento di Chimica "G. Ciamician", via Selmi 2, I-40126 Bologna, Italy. E-mail: francesco.poalucci@unibo.it; Fax: +39-0512099456; Tel: +39-0512099465*
[g]*Friedrich-Alexander-Universität Erlangen-Nürnberg Universität Erlangen, Department of Chemistry and Pharmacy & Interdisciplinary Center for Molecular Materials (ICMM), Egerlandstrasse 3, D-91058 Erlangen, Germany. E-mail: guldi@chemie.uni-erlangen.de; Fax: +49-(0)9131/85-28307; Tel: +49-(0)9131/85-27341*

† This paper is part of a *Journal of Materials Chemistry* theme issue on carbon nanostructures.

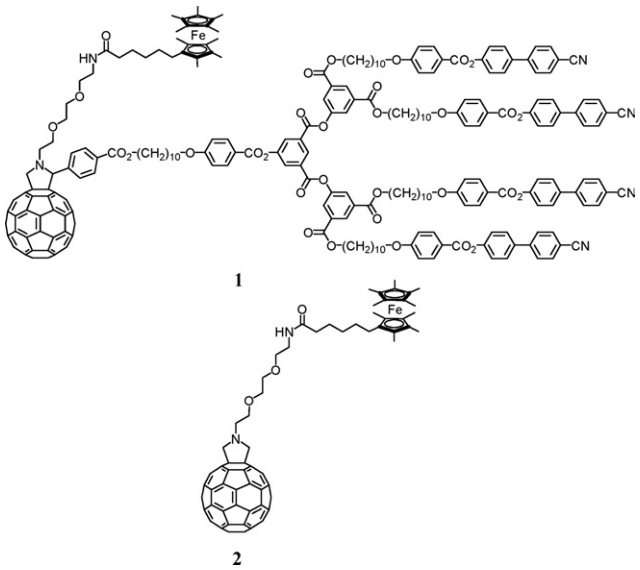

Fig. 1 Structures of the liquid-crystalline fullerene-ferrocene dyad **1** and model compound **2**.

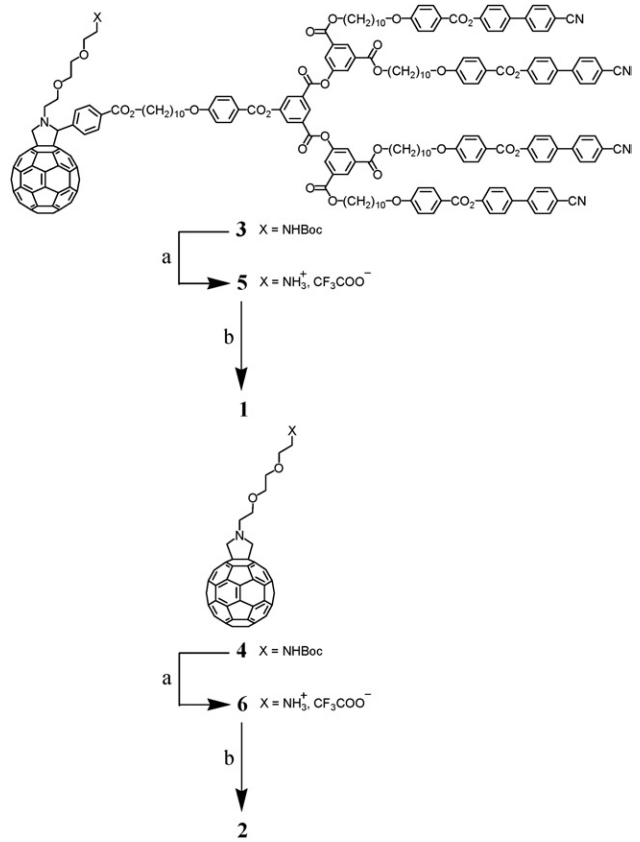

Scheme 1 (a) Trifluoroacetic acid (TFA), CH_2Cl_2, rt, 1 h, **5** 95%, **6** quantitative. (b) **7**, Et_3N, EDC, HOBT, CH_2Cl_2, rt, overnight, **1** 38%, **2** 39%.

carboxaldehyde **8**[23,24] with (4-carboxybutyl)triphenylphosphonium bromide under Wittig reaction conditions. The double bond of the acid derivative **9** was then hydrogenated in the presence of Pd/C to give the ferrocene derivative **7** (Scheme 2).

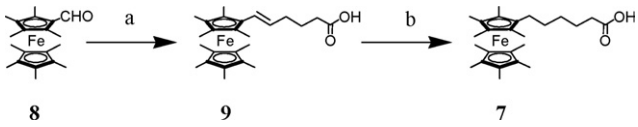

Scheme 2 (a) *t*BuOK, (4-carboxybutyl)triphenylphosphonium bromide, THF, rt, 3.5 h, 57%. (b) H_2, Pd/C, CH_2Cl_2–EtOH, rt, 7 h, quantitative yield.

Liquid-crystalline properties

The thermal and liquid-crystalline properties of compound **1** were investigated by polarized optical microscopy (POM) and differential scanning calorimetry (Table 1). The C_{60}–Fc* derivative **1** showed a smectic A phase which was identified by POM from the observation of focal-conic and homeotropic textures (Fig. 2). The clearing point of **1** is significantly lower than that of the liquid-crystalline aldehyde precursor (*ca.* 185 °C) but remains very close to the clearing point of the *N*-methyl fulleropyrrolidine containing the dendrimer of second-generation (*ca.* 168 °C).[25] This shows that despite its size, the peralkylated ferrocene does not significantly destabilize the mesophase. By analogy with our former studies on liquid-crystalline C_{60}–Fc dyads,[16] we can assume that the supramolecular organization is governed by steric factors, *i.e.* the necessary adjustment between the cross section of C_{60} and of the four cyanobiphenyl mesogens (see Fig. 1 in ref. 16).

Photophysical properties

A series of photophysical measurements was carried out with **1** and **2** in three different solvents: anisole, THF, and benzonitrile. Complementary measurements with a *N*-methylfulleropyrrolidine[26] were also performed, which served as reference experiments.

Table 1 Phase-transition temperatures[a] of **1**

Compound	T_g/°C	Transition	Temperature/°C	ΔH/kJ mol^{-1}
1	57	SmA → I	155	14.9

[a] T_g = glass transition temperature, SmA = smectic A phase, I = isotropic liquid. Temperatures are given as the onset of the peaks obtained during the second heating run; the T_g was determined during the first cooling run.

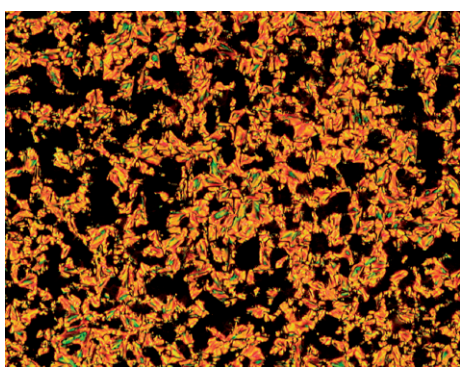

Fig. 2 Thermal–polarized optical micrograph of the focal-conic fan and homeotropic textures displayed by **1** in the smectic A phase at 153 °C.

Optical absorption spectra of **1** and **2** consist in the visible range of two major absorption bands, that is, one at 329 nm and one at 432 nm. Both bands match those seen in the *N*-methylfulleropyrrolidine model compound. Particularly important are the low energy absorptions—around 432 nm—which have evolved as a characteristic feature of 1,2-adducts of C_{60}.

Excited state behavior of **1** and **2** was first investigated by steady-state and time-resolved fluorescence measurements upon exciting the fullerene moiety at 325 nm. At first glance, a marked quenching of the fullerene centered emission—around 715 nm—is seen when comparing the steady-state fluorescence of **1** and **2** with that of the *N*-methylfulleropyrrolidine model compound (Fig. 3). This general trend holds in all the tested solvents and seems to undergo amplification in the more polar solvents. A closer analysis reveals red-shifted fluorescence in the two dyads. From these observations we conclude that the electron donating ferrocene triggers an efficient deactivation of the fullerene singlet excited state. The influence of the mesogenic unit in **1** becomes apparent in the fluorescence quenching. Lower fluorescence quantum yields—*ca.* 20%—prompt faster electron transfer kinetics (Table 2).

The fluorescence decay measurements shed light onto the aforementioned considerations in a more quantitative manner. In particular, they allow monitoring of the dynamics of the charge-separation process. The fluorescence time profile for the *N*-methylfulleropyrrolidine reference displays a single-exponential decay, from which a lifetime of 1.3 ± 0.05 ns was estimated. In contrast, in dyads **1** and **2** the major decay components exhibit values of 0.22 ± 0.03 ns.

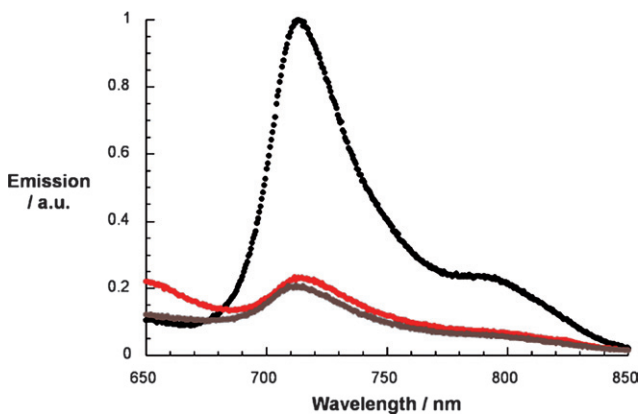

Fig. 3 Steady-state fluorescence spectra in anisole of *N*-methylfulleropyrrolidine (black spectrum), liquid-crystalline dyad **1** (brown spectrum) and dyad **2** (red spectrum) with matching absorption at the excitation wavelength of 325 nm.

Finally, transient absorption measurements were carried out to confirm the fast fullerene singlet excited state deactivation and, in addition, to characterize the nature of the photoproducts. In the *N*-methylfulleropyrrolidine reference the singlet excited state—displaying a distinctive singlet–singlet transition around 880 nm—is formed instantaneously, which undergoes a quantitative intersystem crossing (5×10^8 s^{-1}) to yield the long-lived triplet manifold. Characteristics of the latter are maxima at 360 and 700 nm, followed by a low energy shoulder at 800 nm. In contrast, the femtosecond transient absorption measurements with **1** (Fig. 4) and **2** (Fig. 5) revealed that the fullerene singlet excited state transforms rapidly into a radical ion pair state instead of slow intersystem crossing. Spectral characteristics of

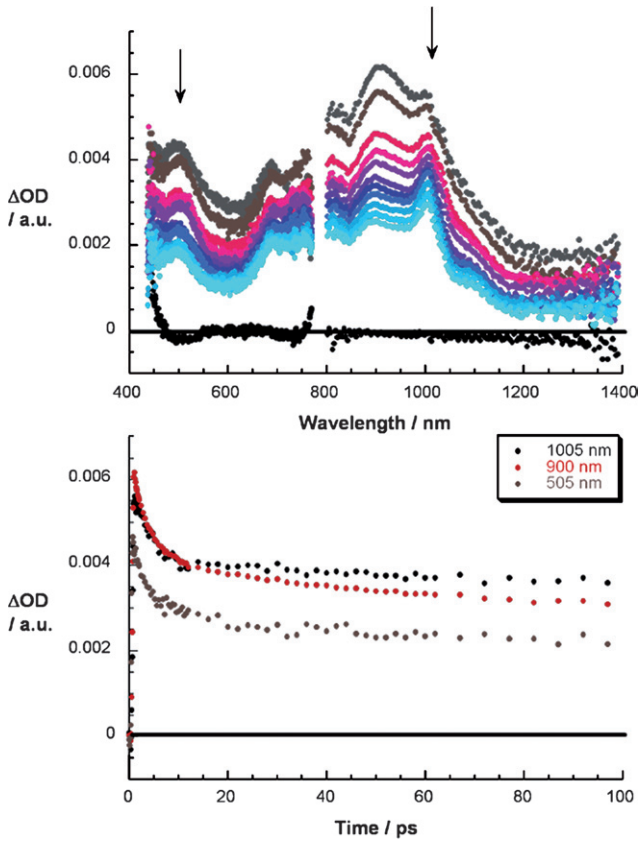

Fig. 4 Upper part: differential absorption spectra (visible and near-infrared) obtained upon femtosecond flash photolysis (387 nm) of **1** (~1 × 10^{-5} M) in nitrogen saturated THF solutions with several time delays between 0 and 50 ps at room temperature—arrows indicate the spectral evolution. Lower part: time-absorption profiles of the spectra shown above at 505, 900, and 1005 nm, monitoring the decay of the singlet excited state.

Table 2 Photophysical properties of dyads **1** and **2**

Solvent	Fluorescence quantum yield (Φ) of compound **2**	Fluorescence quantum yield (Φ) of compound **1**	Fluorescence quantum yield (Φ) of the *N*-methyl fulleropyrrolidine
THF	2.478×10^{-4}	1.836×10^{-4}	6.0×10^{-4}
Toluene	1.884×10^{-4}	1.938×10^{-4}	6.0×10^{-4}
Benzonitrile	2.424×10^{-4}	3.792×10^{-4}	6.0×10^{-4}
Anisol	2.322×10^{-4}	2.496×10^{-4}	6.0×10^{-4}

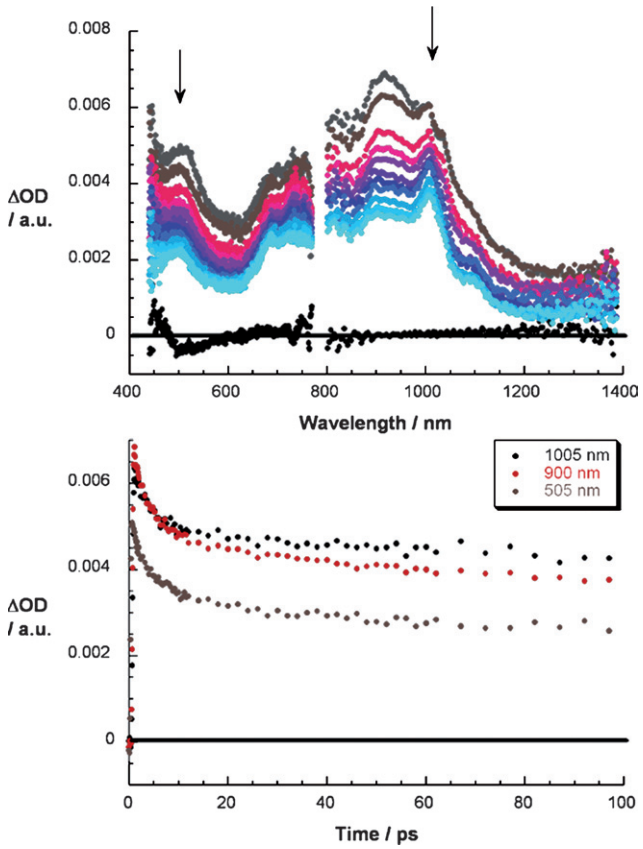

Fig. 5 Upper part: differential absorption spectra (visible and near-infrared) obtained upon femtosecond flash photolysis (387 nm) of **2** ($\sim \times 10^{-5}$ M) in nitrogen saturated THF solutions with several time delays between 0 and 50 ps at room temperature, arrows indicate the spectral evolution. Lower part: time-absorption profiles of the spectra shown above at 505, 900, and 1005 nm, monitoring the decay of the singlet excited state

the radical ion pair state include fingerprint absorptions of the one-electron reduced fullerene radical anion in the near-infrared—at 1000 nm—and in the visible—at 500 nm. Spectral support for the one-electron oxidized form of ferrocene should be found in the 600 to 700 nm range, for which, however rather low extinction coefficients are reported: 500 l mol^{-1} cm^{-1} at 625 nm. In the case of the radical ion pair states for **1** and **2** the particular wavelength range is dominated by contributions that stem from the fullerene radical anion.

Electrochemistry

The cyclic voltammetric (CV) behavior of **1** and of reference compound **2** (Fig. 6) were investigated in THF solutions under strictly aprotic conditions.[27] The CV curve relative to a 0.5 mM **1** THF solution, at 25 °C and at a scan rate of 1.0 V s^{-1}, shown in Fig. 6, displays a series of subsequent reduction peaks which were in part attributable to the fulleropyrrolidine moiety while the remaining ones were attributed to the dendrimer.

In particular, peaks located at −0.47, −1.00 and −1.61 V ($E_{1/2}$) are typical of fulleropyrrolidines studied under similar conditions,[28] and, on the basis of comparison with model compound **2**, were therefore attributed to the subsequent reversible

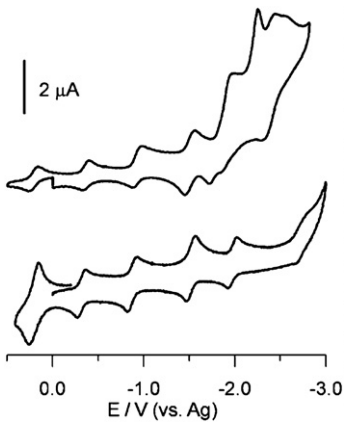

Fig. 6 CV curves of **1** (0.5 mM) (top curve), and **2** (0.5 mM) (bottom curve) in THF (0.05 M TBAH), at 25 °C and a scan rate of 1 V s^{-1}.

reductions of the fullerene unit in **1**. At odds with fulleropyrrolidines, the peak at −1.61 V comprises two electrons, thus suggesting the occurrence of two one-electron reduction processes, fortuitously located at very close potentials, one centered in the fullerene moiety, the other one in the dendritic part. A similar behavior was in fact also observed in the analogous C_{60}-Fc dendrimer investigated under similar conditions.[16] At more negative potentials, the CV curves of **1** are characterized by intense (and only partly reversible) reduction peaks also attributed to the dendrimer moiety. In fact, such a moiety contains various functional groups that are capable of undergoing reduction processes at such negative potentials, namely the four equivalent cyanobiphenyl groups and the three equivalent isophtaloyl ester groups present in the dendritic core.[25] On the other hand, the fulleropyrrolidine **2** also undergoes another two reduction peaks in this potential region, at −2.10 and −2.85 V, respectively, that in the case of **1** are superimposed on those associated to the reduction of the dendritic units. Finally, the oxidation peak observed in the positive potential region is associated with the one-electron oxidation of the peralkylated ferrocene moiety. Such an oxidation is located at 0.10 V in both compounds, *i.e.* about 600 mV less positive than oxidation of ferrocene in C_{60}-Fc dendrimer.[16]

Conclusions

We described the synthesis, characterization and photophysical properties of two fulleropyrrolidines bearing a nonamethylferrocene. Fullerene derivative **1** was designed to display mesomorphic properties (presence of a cyanobiphenyl-based dendrimer) while fulleropyrrolidine **2** served as a reference compound to evaluate the influence of the liquid-crystalline dendron on the electrochemical and photophysical properties. We demonstrated that the introduction of a non-mesogenic group like nonamethylferrocene **7** does not alter the supramolecular organization governed by the cyanobiphenyl groups. The two dyads gave interesting photoinduced electron transfer phenomena. The photophysical properties of **1** and **2** were investigated by steady-state and time-resolved fluorescence as well as transient absorption spectroscopy in polar and apolar solvents. We demonstrated that the fluorescence of the fullerene unit is quenched in **1** and **2** compared to the *N*-methylfulleropyrrolidine used as reference.

Femtosecond transient absorption permitted us to identify the formation of the radical anion of the fullerene. Oxidation and reduction processes were investigated by cyclic voltammetry, and were in agreement with the electrochemical characteristics of the redox-active units (peralkylated ferrocene, fullerene, dendrimer).

Experimental

General methods

Transition temperatures (onset point) and enthalpies were determined with a differential scanning Mettler DSC 822 calorimeter, under N_2/He, at a rate of 10 °C min^{-1}. Optical studies were conducted using a Zeiss-Axioscope polarizing microscope equipped with a Linkam-THMS-600 variable-temperature stage under N_2.

The one-compartment electrochemical cell was of airtight design with high-vacuum glass stopcocks fitted with either Teflon or Viton O-rings in order to prevent contamination by grease. The connections to the high-vacuum line and to the Schlenck containing the solvent were obtained by spherical joints also fitted with Viton O-rings. The pressure measured in the electrochemical cell prior to performing the trap-to-trap distillation of the solvent was typically 1.0 to 2.0 $\times$ 10^{-5} mbar. The working electrode was a Pt disc electrode (diameter: 125 mm) sealed in glass. The counter electrode consisted of a platinum spiral and the quasi-reference electrode was a silver spiral. The quasi-reference electrode drift was negligible for the time required by a single experiment. Both the counter and reference electrodes were separated from the working electrode by ~0.5 cm. Potentials were measured with respect to a ferrocene standard, and are always referred to a saturated calomel electrode (SCE). $E_{1/2}$ values correspond to $(E_{pc} + E_{pa})/2$ from cyclic voltammetry (CV) (E_{pc} and E_{pa}: cathodic and anodic peak potentials). Ferrocene was also used as an internal standard for checking the electrochemical reversibility of a redox couple. Voltammograms were recorded with an AMEL Model 552 potentiostat or a custom made fast potentiostat controlled by either an AMEL Model 568 function generator or an ELCHEMA Model FG-206F. Data acquisition was performed by a Nicolet Model 3091 digital oscilloscope interfaced to a PC. Temperature control was accomplished within 0.1 μC with a Lauda thermostat.

Steady-state emission and excitation spectra were recorded with a FluoroMax-3 (Horiba Company). Time-resolved emission fluorescence lifetimes were measured with a Laser Strope Fluorescence Lifetime Spectrometer (Photon Technology International) with 337 nm laser pulses from a nitrogen laser fiber-coupled to a lens-based T-formal sample compartment equipped with a stroboscopic detector. Details of the Laser Strobe systems are described on the manufacturer's web site (http://www.pti-nj.com). Fluorescence spectra were measured at room temperature. Femtosecond transient absorption studies were performed with 387 nm laser pulses (1 kHz, 150 fs pulse width) from an amplified Ti:sapphire laser system. Picosecond laser flash photolysis experiments were carried out with 355 nm laser pulses from a mode-locked, Q-switched Quantel YG-501 DP Nd:YAG laser system (pulse width 18 ps, 2–3 mJ per pulse).

FT-IR spectra were recorded on Jasco spectrophotometer FT-IR-200 using KBr powder (DRIFT system). UV spectra were recorded on a Varian Cary 5000 spectrophotometer. ^1H and ^{13}C spectra were recorded on a Varian Gemini-200 or on a Bruker AMX-400 spectrometer with tetramethylsilane (TMS) as the internal standard. Chemical shifts are given in ppm relative to that of tetramethylsilane. Elemental analyses were done at the University of Geneva (Pharmaceutical Chemistry Laboratory). Abbreviations: column chromatography = CC; 1-(3-dimethylaminopropyl)3-ethylcarbodiimide hydrochloride = EDC; 1-hydroxybenzotriazole = HOBT.

Materials and synthesis

[60]Fullerene was purchased from Bucky-USA (99.5%), and all other reagents and solvents were used as purchased from Fluka, Aldrich, Acros, Riedel-de-Haën, J. T. Baker and Cambridge Isotope Laboratories. For the syntheses, THF (potassium, under N_2) were distilled prior to use. The silica gel NM Kieselgel 60 (70-230 mesh ASTM) was obtained from Macherey-Nagel and was used as the support for any column chromatography. Compounds **3**,[16] **4**,[22] **5**,[16] **6**[22] and **8**[23,24] were prepared according to the literature procedures.

Compound 9

A solution of *t*BuOK (8.24 g, 73 mmol) in dry THF (40 ml) was added dropwise to a mixture of (4-carboxybutyl)triphenylphosphonium bromide (13.03 g, 29 mmol) and dry THF (50 ml). The solution was stirred at rt for 30 min and 1-formylnonamethylferrocene (5 g, 15 mmol) in dry THF (50 ml) was added dropwise. The mixture was stirred at rt for 3 h and evaporated to dryness. Diethyl ether (250 ml) and NaOH 5 M (150 ml) were added. The aqueous layer was treated with HCl 2 M until pH = 2, then extracted three times with ethyl acetate. The organic layers were combined, dried ($MgSO_4$) and evaporated to dryness. Purification of the residue by CC (hexane–acetone: 2 : 1) gave a dark yellow powder (3.57 g, 57%). ^1H NMR (acetone-d_6): δ = 5.80–5.60 (m, 2H, *C*H=CH), 2.36 (t, J = 7.3 Hz, 2H, *CH_2*CO_2H), 2.11 (m, 2H, CH=CH-*CH_2*), 1.73 (m, 2H, *CH_2*–CH_2–CO_2H), 1.47 (s, 6H, 2 CH_3), 1.41 (s, 6H, 2 CH_3), 1.33 (s, 15H, 5 CH_3). Anal. calcd for $C_{25}H_{36}O_2Fe$ (424.41): C, 70.75; H, 8.55. Found: C, 70.78; H, 8.57%.

Compound 7

A mixture of nonamethylferrocene-1-(5-hexenoic) acid (1.12 g, 2.65 mmol), Pd/C (20%) (0.23 g) in CH_2Cl_2 (20 ml preliminary passed on basic alumina) and a few ml of ethanol was stirred at rt for 7 h under H_2 (4 bar). The mixture was filtered through celite and evaporated to dryness. Purification of the solid residue by CC (diethyl ether) gave a yellow powder (1.11 g, quantitative yield). ^1H NMR (acetone-d_6): δ = 2.30 (t, J = 7.1 Hz, 2H, *CH_2*CO_2H), 2.09 (t, J = 7 Hz, 2H, *CH_2*–Cp), 1.62 (m, 2H, *CH_2*–CH_2–CO_2H), 1.47 (s, 6H, 2 CH_3), 1.42 (s, 6H, 2 CH_3), 1.32 (s, 15H, 5 CH_3), 1.32–1.10 (m, 4H, 2 CH_2). ^{13}C NMR (acetone-d_6): δ = 174.23, 80.86, 65.62, 54.47, 33.77, 30.21, 29.93, 29.73, 29.54, 29.35, 29.16, 28.96, 28.77, 25.24, 8.89. Anal. calcd for $C_{25}H_{38}O_2Fe$ (426.42): C, 70.42; H, 8.98. Found: C, 70.51; H, 9.07%.

Compound 1

A solution of carboxylic acid **7** (23 mg, 0.034 mmol), EDC (13 mg, 0.068 mmol) and HOBT (9 mg, 0.068 mmol) in CH_2Cl_2 (2 ml) was stirred at rt for 15 min and then added dropwise to a suspension of **5** (97 mg, 0.027 mmol) and Et_3N (8.2 ml, 0.054 mmol) in CH_2Cl_2 (2 ml). The mixture was stirred at rt for 3 h. The product was purified by CC (toluene–ethyl acetate 8 : 2), and then precipitated from CH_2Cl_2 solution using diethyl ether. Yield: 38% (41 mg, 0.010 mmol). ^{1}H NMR ($CDCl_3$): $\delta = 8.91$ (t, $J = 1.5$ Hz, 1H), 8.61 (t, $J = 1.5$ Hz, 2H), 8.33 (d, $J = 1.5$ Hz, 2H), 8.20–8.02 (m, 16H), 7.89 (d, $J = 8$ Hz, 2H), 7.77–7.54 (m, 24), 7.35–7.22 (m, 8H), 7.01–6.89 (m, 10H), 5.89 (t, $J = 5.4$ Hz, 2H), 5.20 (s, 1H), 5.19 (d, $J = 9.5$ Hz, 1H), 4.43–4.19 (m, 11H), 4.11–3.89 (m, 12H), 3.81–3.65 (m, 4H), 3.63–3.53 (m, 2H), 3.51–3.29 (m, 3H), 2.96–2.79 (m, 1H), 2. 13 (t, $J = 7.6$ Hz, 2H), 2.08–1.95 (m, 2H), 1.88–1.09 (series of m, 113H). ^{13}C NMR ($CDCl_3$): δ = 173.06, 166.38, 146.87, 164.80, 164.43, 164.09, 163.69, 163.07, 156.16, 153.93, 152.91, 151.60, 150.55, 147.31, 146.52, 146.28, 146.20, 145.96, 145.56, 145.35, 145.28, 144.86, 144.34, 143.02, 142.72, 142.60, 142.43, 142.02, 141.83, 141.54, 140.26, 139.88, 136.70, 136.42, 135.96, 135.60, 132.68, 132.37, 131.15, 130.73, 129.92, 129.51, 129.12, 128.37, 127.71, 127.06, 122.60, 121.25, 120.35, 118.92, 114.60, 114.41, 111.05, 82.11, 78.93, 76.08, 70.62, 70.47, 70.22, 69.32, 68.43, 67.83, 65.97, 65.38, 52.34, 39.29, 36.92, 29.83, 29.56, 29.46, 29.36, 29.22, 28.77, 26.10, 25.90, 9.59. IR-DRIFT (KBr): 3425, 3075, 2927, 2849, 2217, 1729, 1602, 1506, 1252, 1062, 1009, 840, 756, 547, 478 cm^{-1}. UV-Vis (CH_2Cl_2): λ_{max}. 272, 330, 431, 699.

Compound 2

A solution of carboxylic acid **7** (35 mg, 0.082mmol), EDC (31 mg, 0.164 mmol) and HOBT (22 mg, 0.164 mmol) in CH_2Cl_2 (11 ml) was stirred at rt for 15 min under N_2. Then, a suspension of **6** (100 mg, 0.099 mmol) and Et_3N (27 ml, 0.197 mmol) in CH_2Cl_2 (11 ml) was added dropwise and the mixture was stirred at rt overnight. The product was purified by CC (toluene–ethyl acetate 8 : 2), and then precipitated from CH_2Cl_2 solution using methanol and diethyl ether. Yield: 39% (42 mg, 0.032 mmol). ^{1}H NMR ($CDCl_3$): $\delta = 5.99$ (t, $J = 5.4$ Hz, 1H), 4.49 (s, 4H), 4.04 (t, $J = 5.4$ Hz, 2H), 3.84–3.68 (m, 4H), 3.60 (t, $J = 5.0$ Hz, 2H), 3.53–3.41 (m, 2H), 3.35 (t, $J = 5.4$ Hz, 2H), 2.16 (t, $J = 7.5$ Hz, 2H), 2.12–1.98 (m, 2H), 1.80–1.48 (m, 27H), 1.41–1.13 (m, 6H). ^{13}C NMR ($CDCl_3$): δ = 173.10, 154.96, 147.33, 146.27, 146.09, 146.02, 145.69, 145.43, 145.32, 144.58, 143.15, 142.66, 142.23, 142.09, 141.92, 140.19, 136.22, 78.92, 78.79, 78.27, 70.86, 70.62, 70.55, 70.47, 70.19, 68.66, 54.44, 39.32, 36.97, 31.06, 29.84, 25.92, 25.32, 9.63. IR-DRIFT (KBr): 2897, 1669, 1432, 1371, 1110, 1027, 762, 521, 433. cm^{-1}. UV-Vis (CH_2Cl_2): λ_{max}. 256, 329, 430, 703. ES-MS, THF–MeOH 1 : 1): *m*/*z* 1302 (MH+).

Acknowledgements

This work was carried out with partial support from the University of Trieste, INSTM, MUR (PRIN 2006, prot. 20064372 and Firb, prot. RBNE033KMA), the EU (RTN networks "WONDERFULL" and "FAMOUS"), SFB 583, DFG (GU 517/4-1), FCI, the Office of Basic Energy Sciences of the U. S. Department of Energy, and the Swiss National Science Foundation (grant no. 200020-103424). RD acknowledges the Swiss National Science Foundation for financial support (grant no. 200020-111681). MP and DG thank the Vigoni program for travel support.

References

1 H. Imahori, *Bull. Chem. Soc. Jpn.*, 2007, **80**, 621.
2 H. Imahori and T. Umeyama, in *Fullerenes: Principles and Applications*, ed. F. Langa and J.-F. Nierengarten, RSC Publishing, Cambridge, 2007, pp. 266–300.
3 S. Campidelli, A. Mateo-Alonso and M. Prato, in *Fullerenes: Principles and Applications*, ed. F. Langa and J.-F. Nierengarten, RSC Publishing, Cambridge, 2007, pp. 191–220.
4 D. Bonifazi, O. Enger and F. Diederich, *Chem. Soc. Rev.*, 2007, **36**, 390.
5 D. Felder, B. Heinrich, D. Guillon, J.-F. Nicoud and J.-F. Nierengarten, *Chem.–Eur. J.*, 2000, **6**, 3501.
6 M. Kimura, Y. Saito, K. Ohta, K. Hanabusa, H. Shirai and N. Kobayashi, *J. Am. Chem. Soc.*, 2002, **124**, 5274.
7 M. Sawamura, K. Kawai, Y. Matsuo, K. Kanie, T. Kato and E. Nakamura, *Nature*, 2002, **419**, 702.
8 Y. Matsuo, A. Muramatsu, R. Hamasaki, N. Mizoshita, T. Kato and E. Nakamura, *J. Am. Chem. Soc.*, 2004, **126**, 432.
9 Y. Matsuo, A. Muramatsu, Y. Kamikawa, T. Kato and E. Nakamura, *J. Am. Chem. Soc.*, 2006, **128**, 9586.
10 R. Deschenaux, B. Donnio and D. Guillon, *New J. Chem.*, 2007, **31**, 1064.
11 J. Lenoble, S. Campidelli, N. Maringa, B. Donnio, D. Guillon, N. Yevlampieva and R. Deschenaux, *J. Am. Chem. Soc.*, 2007, **129**, 9941.
12 C. Bingel, *Chem. Ber.*, 1993, **126**, 1957.
13 M. Maggini, G. Scorrano and M. Prato, *J. Am. Chem. Soc.*, 1993, **115**, 9798.
14 M. Prato and M. Maggini, *Acc. Chem. Res.*, 1998, **31**, 519.
15 M. Even, B. Heinrich, D. Guillon, D. M. Guldi, M. Prato and R. Deschenaux, *Chem.–Eur. J.*, 2001, **7**, 2595.
16 S. Campidelli, E. Vázquez, D. Milic, M. Prato, J. Barberá, D. M. Guldi, M. Marcaccio, D. Paolucci, F. Paolucci and R. Deschenaux, *J. Mater. Chem.*, 2004, **14**, 1266.
17 S. Campidelli, L. Pérez, J. Rodrígez-López, J. Barberá, F. Langa and R. Deschenaux, *Tetrahedron*, 2006, **62**, 2115.
18 S. Campidelli, R. Deschenaux, J.-F. Eckert, D. Guillon and J.-F. Nierengarten, *Chem. Commun.*, 2002, 656.
19 E. Allard, F. Oswald, B. Donnio, D. Guillon, J. L. Delgado, F. Langa and R. Deschenaux, *Org. Lett.*, 2005, **7**, 383.
20 S. Campidelli, R. Deschenaux, A. Swartz, G. M. A. Rahman, D. M. Guldi, D. Milic, E. Vázquez and M. Prato, *Photochem. Photobiol. Sci.*, 2006, **5**, 1137.
21 J. Ruiz and D. Astruc, *C. R. Acad. Sci.*, 1998, **1**, 21.
22 K. Kordatos, T. Da Ros, S. Bosi, E. Vázquez, M. Bergamin, C. Cusan, F. Pellarini, V. Tomberli, B. Baiti, D. Pantarotto, V. Georgakilas, G. Spalluto and M. Prato, *J. Org. Chem.*, 2001, **66**, 4915.
23 A. Z. Kreindlin, S. S. Fadeeva and M. I. Rybinskaya, *Izv. Akad. Nauk SSSR, Ser. Khim.*, 1984, 403.
24 R. Deschenaux, M. Schweissguth, M.-T. Vilches, A.-M. Levelut, D. Hautot, G. J. Long and D. Luneau, *Organometallics*, 1999, **18**, 5553.
25 S. Campidelli, J. Lenoble, J. Barberá, F. Paolucci, M. Marcaccio, D. Paolucci and R. Deschenaux, *Macromolecules*, 2005, **38**, 7915.
26 D. M. Guldi and M. Prato, *Acc. Chem. Res.*, 2000, **33**, 695.
27 F. Paolucci, M. Carano, P. Ceroni, L. Mottier and S. Roffia, *J. Electrochem. Soc.*, 1999, **146**, 3357.
28 S. Cattarin, P. Ceroni, D. M. Guldi, M. Maggini, E. Menna, F. Paolucci, S. Roffia and G. Scorrano, *J. Mater. Chem.*, 1999, **9**, 2743.